Effects of competing interactions on phase transition temperature in the Ising model

Nguyen Thi Kim Oanh*

Faculty of Natural Sciences, Electric Power University, 235 Hoang Quoc Viet, Nghia Do, Hanoi, Vietnam.
*Corresponding author: oanhnt@epu.edu.vn

Received 12 Feb. 2026; Revised 02 Apr. 2026; Accepted 11 May 2026; Published 25 May 2026.
DOI: https://doi.org/10.54939/1859-1043.j.mst.111.2026.95-103

ABSTRACT

This paper focuses on studying the influence of competitive interaction on the phase diagram in a disordered Ising model using the effective field method. The competitive interaction factor is controlled by two parameters, the competition probability p and the fluctuation D. We obtain a phase diagram divided into three distinct regions according to critical temperatures. Specifically, in the range $1 < D < 1.005$ and $D > 1.4$, the system exhibits a single phase transition from ferromagnetic to paramagnetic states. In the range $1.005 \leq D \leq 1.4$, two critical points t_{c1} and t_{c2} are formed corresponding to the AF – FM – PM phase transition sequence. Simultaneously, we observe that the shift of the phase transition temperature depends on the two model parameters (p, D), similar to the effect of doping concentration on the phase transition temperature in the doped manganese perovskites.

Keywords: Disordered Ising model; Doped manganese perovskites; Effective field theory; Phase diagram.

1. INTRODUCTION

Perovskite oxides have garnered significant attention in the research community because of their special magnetic behavior, promising potential in spintronics and sensors, and energy-related technology. The general formula of manganese perovskite oxides is $AMnO_3$, which allows for the substitution of multiple elements, leading to a rich diversity of magnetic properties such as colossal magnetoresistance, magnetocaloric effect, irreversible magnetic effect, and reversal magnetization, etc. It is well known that the competition among different exchange interactions drives the physical properties of these materials. In particular, the most notable are ferromagnetic (FM) and antiferromagnetic (AF) interactions, as known arising from double exchange (DE) and superexchange (SE) between Mn^{3+} and Mn^{4+}. The competition between the different orders makes the system especially sensitive to external perturbations and chemical substitutions. When doped, these compounds exhibit a series of magnetic phase transitions from the paramagnetic (PM) phase to the FM phase at the Curie temperature T_C and to the AF phase at the Néel temperature T_N [1,2]. Thereby, the phase transition temperature can then be easily adjusted by controlling the doping concentration. For instance, Lalitha *et al.* reported that reducing the Cr doping level at the Mn site in $Pr_{0.5}Sr_{0.5}MnO_3$ leads to an increase in the Curie temperature T_C. The effect was attributed to the modification of the Mn^{3+}/Mn^{4+} ratio induced by Cr substitution, which in turn disturbs the balance between FM and AF interactions within the system [3]. Another study demonstrated that doping with Yb at concentrations ranging from $x = 0.02$ to 0.1 in the system $Pr_{0.45-x}Yb_xSr0_{.5}MnO_3$ caused a lattice transformation that could increase the T_C temperature close to room temperature, reaching approximately 302 K, accompanied by a T_N temperature decrease of about 158 K [4]. This behavior is different from the original parent system $Pr_{0.45}Sr_{0.55}MnO_3$, which undergoes a phase transition at T_C of 281 K and T_N of 182 K. Chemical doping not only fundamentally alters the equilibrium between DE and SE interactions but also leads to phase boundary shifts. Therefore, investigating the dependence of the phase transition temperature on doping concentration in competing FM-AF interacting systems is crucial for future technological applications.

Theoretically, the disordered Ising model with competing FM and AF bonds provides a

minimal physically significant framework. In the crystal field, the unoccupied *3d* orbitals of the Mn ion are split into two states as the t_{2g} state and the e_g state. Electrons in the eg region can easily move to empty regions of neighboring ions of different valences. In contract, electrons in the t_{2g} state are localized at the lattice sites. As a result, the spins of the t_{2g} electrons in the Mn ion are considered to be localized spins equivalent to the spins at each lattice site in the Ising model. Furthermore, the Hund's exchange interaction J_H between t_{2g} electrons and flexible electrons e_g is very significantly stronger than the jump kinetic energy t of the eg electron between two nearest neighboring Mn ions ($J_H \gg t$), which greatly reduces the complexity of the original orbital model. In this limit, the spin of the eg electrons is parallel to the direction of the local spin and rotates in the direction of the external magnetic field applied. Therefore, the magnetic order is primarily influenced by the nearest neighbor spin interaction, which is mapped to the nearest neighbor competition model.

In this work, we aim to study the influence of chemical doping on phase transitions in perovskite systems through the competitive interactive Ising model. Doping differences can modify the strength of exchange interactions and redistribute the interaction ingredients. Here, these effects can be related to two control parameters of the model: (i) the probabilities p and $1-p$ representing the density distributions of FM and AF bonds, respectively; and (ii) the fluctuations D related to the intensity of competing interactions.

2. ANALYSIS CALCULATION FOR DISORDERED ISING MODEL

2.1. Ising model with competitive interaction

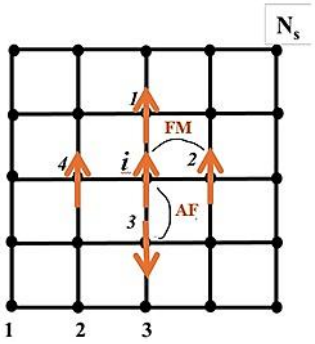

Figure 1. *Cartoon model for Ising model with two types of interactions.*

The Ising model is a simple theoretical framework, but really effective in studying the magnetic properties of disordered material systems [5 - 7]. By incorporating disorder into the exchange interaction parameter among spins, the system's Hamiltonian can be expressed as follows:

$$\mathscr{H} = -\sum_{<i,j>} J_{ij}\sigma_i^z\sigma_j^z - h_e\sum_j \sigma_j^z \qquad (1)$$

Here, $\sigma_i = \pm 1$ is simply the spin at site i, and it is either up (+1) or down (-1). The first term captures the exchange interaction between nearest-neighbor spins, with the strength of that interaction given by J_{ij}. The second term accounts for the interaction energy of the spin system under an external magnetic field h_e. In the present system, positive J_{ij} corresponds to ferromagnetic double-exchange clusters, while negative J_{ij} effectively represents antiferromagnetic superexchange clusters. The interaction J_{ij} follows distribution rules:

$$P(J_{ij}) = p\delta(J_{ij} - J_{FM}) + (1-p)\delta(J_{ij} - J_{AF}) \qquad (2)$$

Where $J_{FM} = J(1+D)$; and $J_{AF} = J(1 - D)$ denote the mean strengths of the FM and AF interactions, occurring with probabilities p and $1-p$, respectively, the parameter J represents the

average value of the exchange integral and is set to unity for convenience. The parameter $D > 1$ characterizes the degree of randomness in the exchange interaction and is a dimensionless quantity. Figure 1 is an example illustrating a competitive Ising model in a 2D lattice with a maximum of 4 nearest neighbors.

2.2. Applying the effective mean-field theory to calculate thermodynamic parameters

To determine the phase diagram and the transition temperature, we utilize an integral transformation for Callen identities and the effective field theory (EFT) [8, 9]. The relative magnetization per site can be obtained by the equation: Readers can see the details of the calculations in Ref. [5]. Within the scope of the present work, we report only the final analytical expressions for the thermodynamic quantities of interest.

The average magnetic moment per lattice site is given by the following expression:

$$m = \left\langle\left\langle \sigma_i \right\rangle\right\rangle_r \tag{3}$$

$$m \simeq \mathrm{Im}\left\{ \int_0^{+\infty} \frac{\exp(ihx/\alpha)}{\sinh\dfrac{\pi x}{2}} \left\{ \sum_{n=0}^{z} C_z^n a^{z-n} (ibm)^n \right\} \right\} \tag{4}$$

Here, the double brackets represent both thermodynamic and random averages. Consequently, the average magnetic moment at each lattice site is obtained as the solution of an algebraic equation that depends on the probability parameter p, the fluctuation strength of the exchange integral D, the inverse temperature α, the external magnetic field h, and the number of nearest neighbors z:

$$m = \sum_{n=0}^{\infty} C_z^n A_n(\alpha, p, D, z, h) m^n \tag{5}$$

Here, C_n^z denotes the combinatorial coefficient, while the coefficient A_n is expressed in integral form:

$$A_n = \int_0^{\infty} \frac{a^{z-n} b^n \sin(\alpha h x + \dfrac{n\pi}{2})}{\sinh(\dfrac{\pi x}{2})} dx \tag{6}$$

The coefficients a and b are defined as:

$$\begin{aligned} a &= p\cos[\alpha(1+D)x] + (1-p)\cos[\alpha(1-D)x] \\ b &= p\sin[\alpha(1+D)x] + (1-p)\sin[\alpha(1-D)x] \end{aligned} \tag{7}$$

The inverse temperature $\alpha = t^{-1} = \dfrac{J}{k_B T}$ and the external magnetic field $h = \dfrac{h_e}{J}$ are dimensionless quantities. Within this framework, the magnetic susceptibility per lattice site, χ, is obtained from the first derivative of the magnetization with respect to the external field:

$$\chi = \frac{\partial m}{\partial h} \tag{8}$$

The internal energy per lattice site is evaluated as the configurational average of the Hamiltonian:

$$E = \left\langle\left\langle \mathscr{H} \right\rangle\right\rangle_r \tag{9}$$

On this basis, the Helmholtz free energy can be determined from the temperature dependence of the internal energy through an integral relation:

$$H(t) = E(t) - t\int_0^t \frac{E(t')}{t'^2}dt' \tag{10}$$

3. RESULTS AND DISCUSSION

3.1. Phase diagram

This work focuses on a disordered model, and all calculations are therefore carried out with the number of nearest neighbors at $z = 4$. In the absence of an external magnetic field, the transition temperature t_c is determined as the solution of the following equation:

$$1 - zA_1(\alpha_c, p, D, z, 0) = 0 \tag{11}$$

with $\alpha_c = \frac{1}{t_c}$.

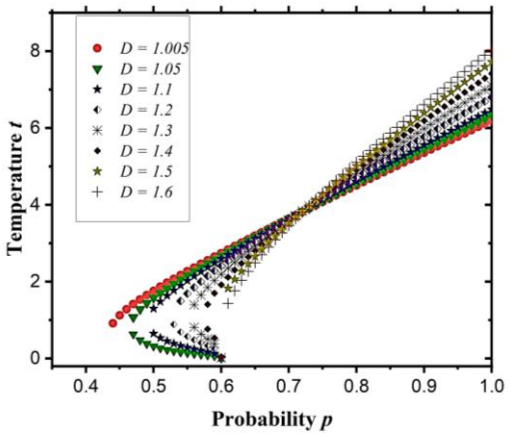

Figure 2. *Phase diagram showing the transition temperature t_c as a function of the probability p for different values of the fluctuation parameter D at h = 0.*

Figure 2 illustrates the dependence of the critical temperature t_c on the probability p for various fluctuating values of D. It can be seen that a phase transition occurs only when the probability p is greater than the critical probability threshold p_c for all values of D, such as with $D = 1.005$, $p_c = 0.44$, or $D = 1.3$, $p_c = 0.53$. It indicates that a sufficiently large number of FM interactions is required to facilitate the formation of magnetic order in the ground state. Here, the phase diagram is divided into three distinct regions. For two regions with a critical temperature point t_c: $D < 1.05$ and $D > 1.4$, the system undergoes a second-order phase transition from the FM to the PM phase in both regions. However, there are some differences in the physical behaviors in the two regions. In the low D region, the phase transition can begin at a low probability at $p_c < 0.5$ ($p = 0.5$ is the probability of equilibrium between FM and AF phases). In this case, the system contains clusters of high-intensity FM, coupled to a background of low-intensity AF. In contrast, in the high D region, where $p_c > 0.5$, the intensity of the AF clusters is significantly enhanced, but they remain isolated amidst a predominance of FM clusters. Importantly, as the probability of the existence of supported FM clusters increases, so does the critical temperature at which the phase transition from FM to PM occurs. This phenomenon is entirely consistent with behavior observed in doped perovskite materials. A notable example is $Pr_{1-x}Ca_xMnO_3$ with $x = 0.25$, 0.27, and 0.29. As the Ca replaces the site of Pr^{3+}, the number of ions Mn^{4+}increases, leading to supporting the AF interactions Mn^{4+}–Mn^{4+}, while the number of FM interactions decreases and weakens and the phase transition temperature T_C is lowered [10]. This phenomenon was also observed in $Pr_{0.5}Sr_{0.5}Mn_{1-x}Cr_xO_3$, where increasing the doping concentration of Cr alters the carrier density of Mn^{3+}/Mn^{4+}, leading to weaker ferromagnetic double exchange interactions, thus a continuous decrease in T_C is

predictable [11]. In the remaining region $1.05 \leq D \leq 1.4$, the system exhibits two critical points, t_{c1} (low) and t_{c2} (high), corresponding to a series of phase transition processes that can be AF– FM – PM. Interestingly, at a specific probability p, when D increases greatly, meaning the J_{AF} interaction strength is enhanced, t_{c1} increases while t_{c2} decreases. This behavior is observed in the magnetic properties of $Pr_{0.5-x}Dy_xSr_{0.5}MnO_3$ [12]. Specifically, Doping Dy^{3+} with a smaller radius than the Pr^{3+} ion, the crystal lattice is distorted, the distance between Mn–O and the Mn–O–Mn angle change subsequently affecting the interaction strength of the DE and SE interaction. Enhancing Dy^{3+} content promotes SE interaction in the AF order, leading to T_N growth and T_C reduction.

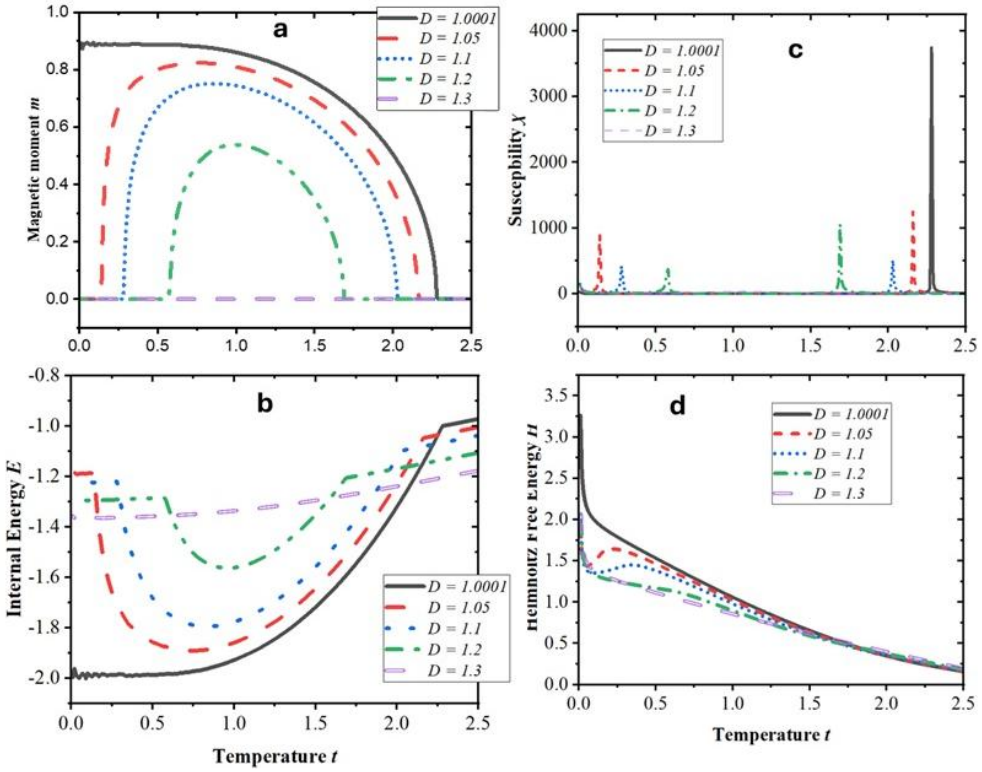

Figure 3. *Temperature dependence of the thermodynamic quantities for different values of the fluctuation parameter at p = 0.55 and h = 0: (a) Magnetic moment m; (b) Internal energy E; (c) Magnetic susceptibility χ; (d) Helmholtz free energy H.*

Figure 3 illustrates the temperature dependence of thermodynamic quantities, including magnetic moment m, internal energy E, magnetic susceptibility χ, and Helmholtz free energy H at $p = 0.55$, $h=0$, with different values of the parameter D. The phase transition is determined at the critical temperature t_c, where the magnetization abruptly drops to 0 (Figure 3a). For D =1.0001, a FM–PM phase transition is observed. However, in the range [1.05 - 1.3], magnetization disappears at two distinct temperatures, indicating the presence of two distinct phase transitions, consistent with the phase diagram in Figure 2. Besides, the phase transition is also reflected in the behavior of an internal energy E (Figure 3b). An internal energy E exhibits a slight linear increase in the disordered phases. In contrast, in the FM phase, the energy E varies significantly and forms a particularly U-shaped curve, beginning at the phase transition points in the [1.05-1.3] region. Similarly, the critical temperature is marked by peaks in magnetic susceptibility χ (Figure 3c). For D = 1.0001, there is only a single peak, while for the interval between 1.05 and 1.3, two peaks correspond to the two critical temperatures t_{c1} and t_{c2}. The free energy $H = E - TS$ decreases nearly linearly to zero above t_c in the PM state, but competing interactions make the entropy change drastically, so H behaves with quite nontrivial features.

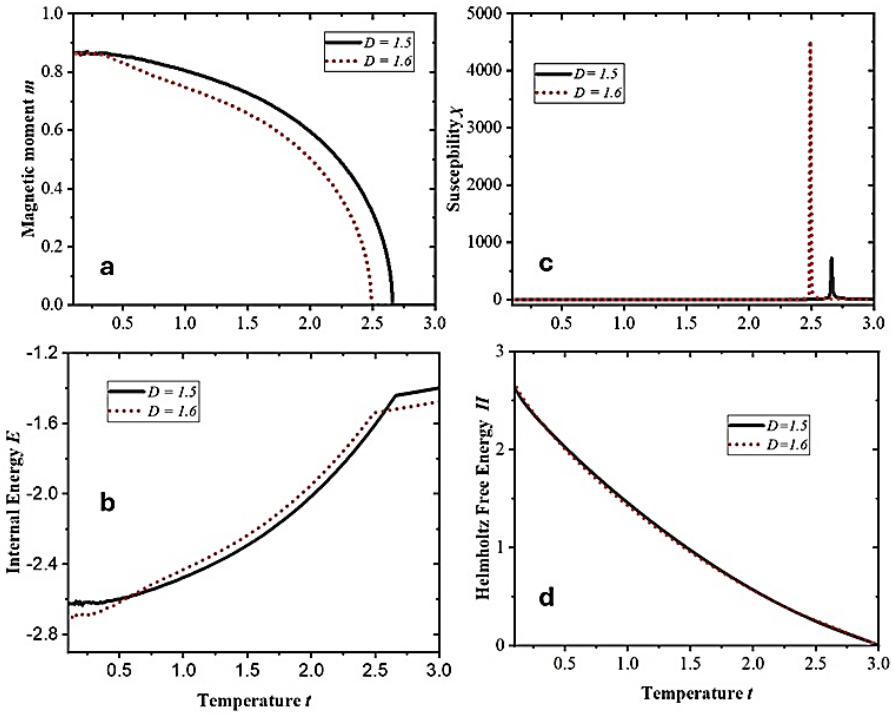

Figure 4. *Temperature dependence of the thermodynamic quantities for different values of the fluctuation parameter D = 1.5 and 1.6 at p = 0.65 and h = 0: (a) Magnetic moment m; (b) Internal energy E; (c) Magnetic susceptibility χ; (d) Helmholtz free energy H.*

Following, the influence of the parameter D on the high-probability region p is investigated through thermodynamic quantities in Figure 4. In this regime, FM interaction predominates, leading the system to undergo only an FM–PM phase transition. As D increases, the contribution from AF clusters also increases, leading to a decrease in the phase transition temperature t_c. The phase transition process is clearly demonstrated by the variation in magnetization m and the internal energy E. Specifically, m decreases to 0. At the same time, E increases, reaching saturation when the system goes to the PM state (as shown in Figure 4a, b). The magnetic sensitivity χ peaks at t_c (Figure 4c) and shifts to a lower temperature with increasing temperature, which indicates a weakening of the FM–PM phase transition. Concurrently, the height of the χ peak reflects a change in critical correlations. The Helmholtz free energy H decreases monotonically from the FM phase to near 0 in the PM phase and depends only weakly on D.

3.2. Influence of the external magnetic field on the thermomagnetic and magnetization curves

In Figure 5, we examine the temperature dependence of the reduced magnetization m under different external magnetic fields h for the case $p = 0.55$. In particular, in the weak-field regime at h = 0.01 and 0.05, the magnetic moment drops to a local minimum, then rises to a peak before plummeting to zero. It can be seen that the system exhibits local AF domains due to high energy degeneracy, so the weak magnetic field is not strong enough to completely orient the spins, leading to domain pinning. As the temperature increases, thermal vibrations disrupt the local AF configurations, and FM will be more dominant. At the higher external fields h = 0.1 and 0.2, the magnetization curve decreases smoothly. because the external field progressively suppresses the AF phase and aligns the spins along its direction. FM-AF competition persists and is insufficient to form complex domain structures at low temperatures. Continuing h up to 0.5, the thermomagnetic curves decrease from the maximum saturated with m = 1. In this case, AF clusters are almost completely suppressed, and the system behaves like a conventional ferromagnetic

system. In addition, increasing the external field broadens the ferromagnetic region. Similar behavior has been reported in doped perovskite systems [12].

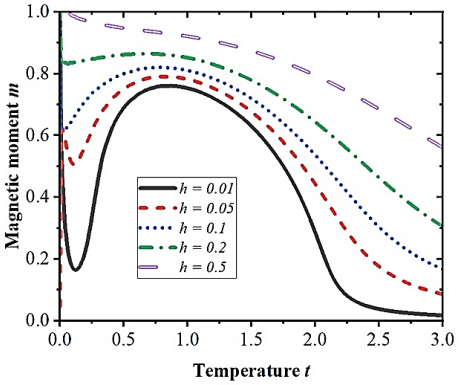

Figure 5. *Thermomagnetic curves measured under different external magnetic fields h at probability p = 0.55 and fluctuation parameter D = 1.1.*

It is obvious that investigating the magnetization curve *m(h)* is essential because it provides powerful evidence to uncover the critical behavior. Figure 6 illustrates the magnetization curves at probability p = 0.55 and fluctuation parameter D = 1.1, examined over the temperature range from t = 0.1 to 3.5 with a temperature step Δt = 0.2. In the range below the transition temperature tc1, the magnetization m increases sharply in the applied magnetic field. The system remains disordered and contains large antiferromagnetic clusters. These clusters tend to reorient under the applied field, gradually driving the system toward a ferromagnetically ordered state. Above t_{c1}, where a stable FM phase is established, the magnetization grows more gradually as the magnetic field increases (Figure 6a). The behavior near the higher transition temperature t_{c2}, is markedly different (Figure 6b). Just below t_{c2}, long-range ferromagnetic order still persists. As a result, the magnetization rises sharply in the low-field region around h = 0.2, and then increases in an almost linear manner as the field becomes stronger. In contrast, above t_{c2},, the magnetization increases linearly from zero with the applied field. This response is characteristic of the paramagnetic phase, where magnetic moments are randomly oriented and only a small fraction aligns with the direction of the external magnetic field.

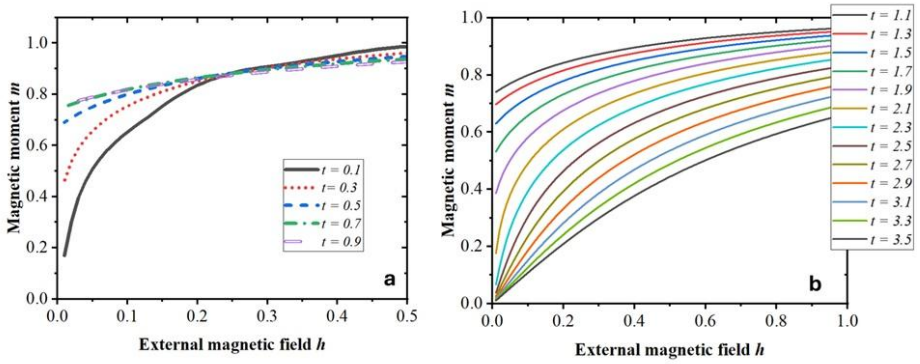

Figure 6. *Magnetization curves at probability p = 0.55 and fluctuation parameter D =1.1 for: (a) The low-temperature region from t = 0.1 to 0.9; (b) The high-temperature region from t = 1.1 to 3.5.*

Theoretical and experimental curves [11] for the sample $Pr_{0.5}Sr_{0.5}Mn_{1-x}Cr_xO_3$ are described in Figure 7. The agreement between the theoretical and experimental results is observed. Interestingly,

the higher the doping concentration, the less FM interaction in the experimental sample. It is similar to the probability reduction p of the FM cluster in the theoretical model. Hence, the microscopic Ising model can be used to explain magnetic properties for the manganese perovskites.

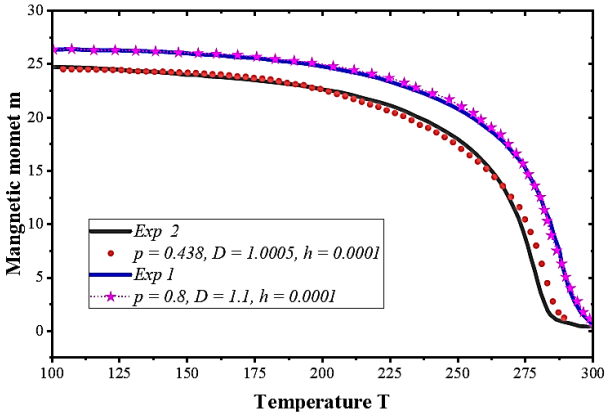

Figure 7. *Fitting curves of magnetization between the disordered Ising model and experiment for sample* $Pr_{0.5}Sr_{0.5}Mn_{1-x}Cr_xO_3$ *: (Exp 1): x = 0.02, (Exp 2): x = 0.05. [11].*

4. CONCLUSIONS

By applying the effective field approximation to the Ising model with competing interactions between two energy levels, we constructed the phase diagram describing the relationship between the transition temperature t_c and the probability p with four nearest neighbors. The thermodynamic quantities, including the magnetization m, internal energy E, magnetic susceptibility χ , and free energy H, were systematically examined in two characteristic regimes: the region where two phase transitions emerge for fluctuations in the range $1.005 \leq D \leq 1.4$ at $p = 0.55$, and the area where only a single FM - PM transition occurs at $p = 0.55$, $D < 1.05$ and $p = 0.6$; $D > 1.4$. The reaction of these thermodynamic parameters in response to temperature and external magnetic field predicted by the theoretical model is consistent with several experimental observations reported for doped perovskite materials. This agreement supports the view that interaction competition plays a central role in the origin of magnetic properties in this class of materials. Especially, when an external magnetic field h differs from 0, the impact of competing interactions becomes even more evident. Here, domain pinning appears in the thermomagnetic curves, and pronounced variations of the magnetization are observed in the magnetization curves, particularly in the low-field region.

Acknowledgement: *This paper presents the results of a science and technology research project funded by Electric Power University in 2024, under project code ĐTKHCN.15/2024.*

REFERENCES

[1]. E. Dagotto et al., "*Colossal magnetoresistant materials: The key role of phase separation*", Physics Reports, Vol. 344, pp. 1-153, (2001).

[2]. N. Chau et al., "*Spin glass-like state, charge ordering, phase diagram and positive entropy change in* $Nd_{0.5-x}Pr_xSr_{0.5}MnO_3$ *perovskites*", Journal of Magnetism and Magnetic Materials, Vol. 303, pp. e402-e405, (2006).

[3]. G. Lalitha et al., "*Magnetocaloric behavior of chromium doped* $Pr_{0.5}Sr_{0.5}MnO_3$ *system*", Physica B: Condensed Matter, Vol. 571, pp. 101-104, (2019).

[4]. R.K. Dokala et al., "*Irreversible metamagnetic transitions in Yb3+ distorted tetragonal* $Pr_{0.45}Sr_{0.55}MnO_3$", Journal of Physics D: Applied Physics, Vol. 57, p. 045001, (2024).

[5]. Giang H. Bach et al., "*First Order Magnetization Process in Polycrystalline Perovskite Manganite*", Materials Transactions, Vol. 56, No. 9, pp. 1320-1322, (2015).

[6]. Oanh K.T. Nguyen et al., "*Fluctuation inducing fractional magnetization behavior on the Shastry–*

Sutherland lattice", Physica B: Condensed Matter, Vol. 583, p. 412012, (2020).
[7]. P. H. Nguyen at al., "*Effective field theory investigation for a disordered Ising model in the description of amorphous magnetic systems*", Journal of Non-Crystalline Solids, Vol. 643, p. 123165, (2024).
[8]. H.B. Callen, "*A note on Green functions and the Ising model*", Physics Letters, Vol. 4, Issue 3, p. 161, (1963).
[9]. B.T. Cong et al., "*Theory of a disordered spin lattice*", J. of Magnetism and Magnetic Materials, Vol. 140-144, Part 1, pp. 259-260, (1995).
[10]. T.A. Ho et al., "*Critical behavior and magnetocaloric effect of* $Pr_{1-x}Ca_xMnO_3$", J. of Applied Physics, Vol. 117, p. 17D122, (2015).
[11]. G. Lalitha et al., "*Magnetocaloric behavior of chromium doped* $Pr_{0.5}Sr_{0.5}MnO_3$ *system*", Physica B: Condensed Matter, Vol. 571, pp. 101-104, (2019).
[12]. Jieyang Fang et al., "*Study on the structural transition and inverse magnetocaloric effect of Dy-substituted* $Pr_{0.5}Sr_{0.5}MnO_3$", Materials Chemistry and Physics, Vol. 323, p. 129626, (2024).

TÓM TẮT

Ảnh hưởng của thăng giáng tác động lên quá trình chuyển pha trong mô hình Ising có cạnh tranh tương tác

Bài báo này tập trung nghiên cứu ảnh hưởng của cạnh tranh tương tác lên giản đồ pha trong mô hình Ising mất trật tự bằng phương pháp trường hiệu dụng. Yếu tố cạnh tranh tương tác được điều khiển biến đổi thông qua hai tham số là xác suất cạnh tranh p và độ thăng giáng D, chúng tôi thu được giản đồ pha phân thành 3 vùng riêng biệt theo nhiệt độ tới hạn. Cụ thể, trong khoảng $1 < D < 1{,}005$ *và* $D > 1{,}4$*, hệ thống biểu hiện một chuyển pha duy nhất từ trạng thái sắt từ sang trạng thái thuận từ. CÒn trong khoảng* $1{,}005 \leq D \leq 1{,}4$*, hai điểm tới hạn tc1 và tc2 hình thành tương ứng với chuỗi chuyển pha AF – FM – PM. Đồng thời, chúng tôi nhận thấy sự dịch chuyển của nhiệt độ chuyển pha phụ thuộc vào hai tham số mô hình (p, D) tương tự như hiệu ứng của nồng độ pha tạp ảnh hưởng lên nhiệt độ chuyển pha trong họ perovskite mangan pha tạp.*

Từ khoá: Mô hình Ising mất trật tự; Perovskite mangan pha tạp; Trường hiệu dụng tương quan; Giản đồ pha.